Manuscript Number:

Title: Acoustic journal bearing - a search for adequate configuration

Article Type: Full Length Article

Keywords: Journal bearing; acoustic levitation; squeeze film mechanism; experimental validation

Corresponding Author: Prof. Tadeusz A Stolarski, PhD; DSc(Eng)

Corresponding Author's Institution: Brunel University

First Author: Tadeusz A Stolarski, PhD; DSc(Eng)

Order of Authors: Tadeusz A Stolarski, PhD; DSc(Eng); Rafal Gawarkiewicz, PhD; Krzysztof Tesch, PhD

Abstract: Classical non-contact bearings are already used in a number of specialist applications. However, there are some specialist areas where they cannot be used for variety of reasons.
The paper presents the search for an optimal configuration of an acoustic journal bearing and shows that the overall shape of the bearing and its geometry are of a vital importance for the load capacity of the bearing. The results presented and discussed in the paper clearly demonstrate that the acoustic journal bearing with appropriate geometry can develop a load capacity of magnitude that can be sufficient for some practical applications.

Suggested Reviewers: Mark Hadfield PhD
Professor, School of Design, Engineering and Computing, Bournemouth University
mhadfield@bournemouth.ac.uk
Well known expert in tribology area.

Gwidon Stachowiak PhD
Professor, Mechanical Engineering, Curtin University
gwidon.stachowiak@curtin.edu.au
Internationally renown researcher in tribology

Ken Mao PhD
Assistant Professor, School of Engineering, University of Warwick
k.mao@warwick.ac.uk
Known for finite element modelling of tribological contacts.

Cover Letter

Dear Editor-in Chief,

I should be grateful for initiating the assessment procedure of our paper entitled 'Acoustic journal bearing – a search for adequate configuration'.

Please let me know the outcome of the review in due time.

Regards,

Tadeusz A Stolarski
Brunel University London

Statement of Originality

On behave of my co-authors, I Tadeusz A Stolarski hereby state:

1   The paper has not been published and is not under consideration for publication.

2   The paper does not contain material which could create any issue of copy write or require permission for reproduction.

Highlights

(i)   The paper demonstrates practical feasibility of an acoustic air bearing.

(ii)   It stresses the importance of the geometrical configuration of the bearing for the acoustic levitation effect.

(iii)   It contains experimental results showing the load capacity of the pressure generated by squeeze film acoustic levitation.

(iv)   Ranks three different geometries of the bearing in accordance with the magnitude of the torque required to initiate motion of the shat for a number of loads on the bearing.

Acoustic journal bearing – a search for adequate configuration

R Gawarkiewicz, T A Stolarski[1], K Tesch

Gdansk University of Technology, Gdansk, Poland

[1] also Brunel University London, United Kingdom

e-mail: mesttas@brunel.ac.uk

Tel: +44(0)1895266693

Abstract: Classical non-contact bearings are already used in a number of specialist applications. However, there are some specialist areas where they cannot be used for variety of reasons. The paper presents the search for an optimal configuration of an acoustic journal bearing and shows that the overall shape of the bearing and its geometry are of a vital importance for the load capacity of the bearing. The results presented and discussed in the paper clearly demonstrate that the acoustic journal bearing with appropriate geometry can develop a load capacity of magnitude that can be sufficient for some practical applications.

Keywords: Journal bearing; acoustic levitation; squeeze film mechanism; experimental validation

1. Introduction

Contactless interaction of objects (with rotational or linear motion) has significant

advantages in many situations. Being non-contact, the systems can be operated at much

higher speeds than using conventional bearings. Also, there should be no problems

associated with overheating and wear of the bearing components. Thus, high precision of

motion and high speed can both be achieved.

Classical non-contact bearings such as aerostatic bearings and magnetic bearings are already

being used in many practical applications. However, a continuous supply of a large volume of

clean air is required for the air bearings, which leads to a high running cost and sometimes a

bulky installation. Magnetic bearings cannot be used for magnetically sensitive

environments due to the strong magnetic flux. It is therefore of a considerable interest to find other concepts for realizing non-contact suspension which can resolve these problems. Acoustic levitation has been found to be a promising alternative solution. It has drawn a significant attention in the last two decades and shown good potentials to overcome some of the shortcomings of the existing non-contact suspension methods [1].

Non-contact bearings based on acoustic levitation use air as lubricant. They share the advantages of classic aerostatic bearings. However, in acoustic levitation the load-carrying pressure is generated internally by means of high frequency mechanical vibrations. Therefore, external supply of pressurized air is not required and the bearing can be very compact. These distinct characteristics make it suitable for certain applications where classic aerostatic or magnet bearings are simply not suitable.

2. Self-levitating bearings

2.1. Standing wave type

Standing wave levitation phenomenon was first observed in 1866 by Kundt during a tube experiment [2], in which small dust particles moved towards the pressure nodes of the standing wave created in a horizontal tube. Solid or liquid objects with effective diameters less than a wavelength can be levitated below the pressure nodes. The axial suspension of an object is an effect of the sound radiation pressure of the standing wave. Combining with a Bernoulli vacuum component, the sound wave can float the objects laterally as well [3].

The first detailed theoretical description of standing wave levitation was given by King [4] and was later extended by Hasegawa and Yosioka [5] to include the effects of compressibility. Embleton [6] adopted King's approach to fit to the case of a rigid sphere in a progressive spherical or cylindrical wave field. Westervelt [7, 8, 9] derived a general

expression for the force owing to radiation pressure acting on an object of arbitrary shape and normal boundary impedance. Westervelt showed that a boundary layer with a high internal loss can lead to forces that are several orders of magnitude greater than those predicted by the classical radiation pressure theory.

A very different approach compared to that of King was presented by Gorkhov [10], who proposed a simple method to determine the forces acting on a particle in an arbitrary acoustic field. The velocity potential was represented as the sum of incident and distributed terms. Barmatz [11] applied Gorkhov's method to derive the generalized potential and force expressions for arbitrary standing wave modes in a rectangular cylindrical and spherical geometries. Xie and Wei [12] studied the acoustic levitation force acting on disk-shaped samples and the dynamics of large water drops in a planar standing wave, by solving the acoustic scattering problem utilising the boundary element method.

2.2. Squeeze film type

In 1964, Salbu [13] reported a levitation system for objects with flat surface. Salbu used magnetic actuators to excite two conforming surfaces oscillating next to each other to generate a positive load supporting force. In 1975, Whymark [14] reported that a brass planar disk of 50 mm in diameter and 0.5 mm in thickness was levitated above a piston vibration source driven harmonically at a frequency of 20 kHz. The levitation effect reported by Salbu and Whymark is named as squeeze film levitation. It is also called near field acoustic levitation.

A schematic diagram of squeeze film levitation system is shown in Fig. 1 [16]. The time-averaged mean pressure in the gap has a value which is higher than the surrounding, caused by the second-order effects possessed by the rapidly squeezed and released gas film

between two plane surfaces. Two distinct properties distinguish this type of levitation from standing wave levitation. Firstly, the reflector is no longer needed; instead, the levitated object itself acts as an obstacle for the free propagation of the ultrasonic wave-front. Secondly, the gap between radiation source and the levitated object must be much smaller than the sound wavelength in air. Thus, instead of a standing wave, a thin gas film is formed between the radiator and the levitated object, which is rapidly squeezed and released.

A simple model introduced by Wiesendanger [15] shows the basic idea of how the squeeze film levitation works. The leaking and pumping at the boundary is neglected in this model and only the trapped gas, rapidly squeezed and released, is considered. Thus the total mass of air in a fixed volume remains constant, resulting in,

$$pV^n \sim ph^n = const$$

where p represents the pressure, V the volume of the trapped gas, h the separation height and n the polytrophic constant (n = 1 for isothermal condition, n = k ≈ 1.4 for adiabatic condition and air). The relation between pressure and levitation distance is nonlinear, which leads to a pressure p(t) resulting from the imposed periodic fluctuation in the separation height h(t). Considering the case shown in Fig. 1 the gap distance oscillates harmonically around an equilibrium position h_0, i.e.

$$h(t) = h_0(1 + \epsilon sin\omega t)$$

in which ω is the angular frequency of the oscillation, ϵ is the fraction a_0/h_0 and denotes the ratio of the vibration amplitude over the mean gap distance, where a_0 is the vibration displacement amplitude. The mean pressure under isothermal condition (n = 1) can be expressed as [15],

$$\bar{p} = \frac{p_0 h_0}{2\pi} \int\limits_{0}^{2\pi} \frac{1}{h(t)} d(\omega t) = \frac{p_0}{\sqrt{1-\epsilon^2}}$$

It can be easily seen that a mean pressure $\bar{p}$ which exceeds the ambient pressure p_0 is obtained. However, to obtain a quantitative result of the levitation pressure, more sophisticated models should be built which takes into account the boundary conditions such as the pressure release at the edge of the gap.

Besides non-contact bearings, squeeze film levitation was also used for non-contact linear transportation systems. In 1998, Hashimoto [17] presented a non-contact transportation system using flexural traveling waves. An aluminium plate was connected to two longitudinal transducers and was driven in a flexural vibration mode by one of the transducers. In order to obtain a traveling wave, one transducer acts as vibration source and the other one as a receiver. The transportation speed can be changed by controlling the vibration amplitude.

In 1964, Salbu [13] first described the concept of constructing a non-contact bearing using squeeze film action. Salbu used magnetic actuators to generate the oscillation and the operating frequency was in the audible range, therefore the bearing was extremely noisy. In the later publications on squeeze film levitation, piezoelectric transducers of various shapes were commonly used to generate the squeeze action effectively. Several designs of squeeze film bearings using bulk piezoelectric ceramics can be found in the U.S. patents invented by Warnock [18], Farron [19], Emmerich [20].

These designs used bulky piezoelectric materials to create uniform vibration amplitude over the entire bearing surfaces. Therefore the transducers were rather massive and required high power to generate sufficient vibration amplitude. Scranton [21] suggested using bending piezoelectric elements to excite a flexural vibration mode of the bearing.

This led to a very compact system design and much lower power dissipation. However, in Scranton's patent, only the basic concept is sketched, and there was no concrete implementation presented.

The model of squeeze film levitation can be constructed by following two different routes: acoustic radiation pressure theory and gas film lubrication theory [22]. The first one modifies the acoustic radiation pressure theory according to the different physical conditions in squeeze film levitation; the second one starts from the theory of gas film lubrication. Gas film lubrication has been investigated for many years in micro-mechanical systems typically by solving Reynolds equation [23].

The important practical application of squeeze film acoustic levitation is to develop non-contact bearings for linear and rotational motion. This is the major concern of this paper in which emphasise is placed on rotational motion.

3. Motivation and aim of the research presented

Research project which selected results are presented in this paper is inspired by the fact that acoustic journal bearings have been found to be a new and attractive alternative for traditional non-contact aerostatic and magnetic bearings. They can potentially find applications in many specialist areas of engineering, especially there where high precision of motion, high speed, and low frictional losses are essential. This is especially true for journal bearings using squeeze film ultrasonic levitation. A number of prototype non-contact suspension and transportation systems based on squeeze film levitation have been reported [13, 15, 21, 24, 25, 26]. However, not many attempts have been made to design a journal bearing operating on a squeeze film acoustic levitation because in this type of a bearing there is a need to generate a high frequency vibration of the bearing surface. This is further

complicated because the surface subjected to high frequency vibration in a journal bearing is circular. Therefore, the geometry of the journal bearing and its overall configuration are both of utmost importance for the effective operation of the acoustic journal bearing. Thus, the main aim of the research presented in this paper was the quest for the optimal geometric configuration of the bearing and testing its effectiveness in generating squeeze film acoustic pressure.

4. Search for optimal configuration

In the search for the most effective, in terms of acoustic pressure generation, geometric configuration of the journal bearing a number of different geometries were considered. This was carried out with the help of finite element programme enabling close examination of the modal shapes generated by piezo-electric transducers (PZT) attached to the bearing shell at different locations and operating and different frequencies. As a result of that three configurations of the acoustic journal bearing with the potential for effective operation (as judged by the modal shapes) were selected for experimental testing which consisted in finding out their load carrying capacity.

4.1. First configuration

The first configuration selected for experimental testing is shown in Fig.2. The nominal bore diameter is 30 mm, thickness of the wall 2 mm, and overall length equal to 50 mm. The overall shape is quite simple and does not require any special manufacturing processes. Aluminium alloy was used for fabrication. Three foil type PZTs were attached to be bearing's

shell as indicated in Fig.2. Forces generated by PZTs, when modulated current flows through them, caused elastic deformation of the bearing.

Radial elastic deformations of the bearing produced by PZTs powered by modulated current of 95 V are shown in Fig. 3. It can be seen that initial circular bore is transformed into 3-lobe shape. This deformed shape is believed to be beneficial for the squeeze film acoustic levitation. A closer view of the bearing's bore deformation is shown in Fig. 4. Again, transformation from a perfect circle to a 3-lobe shape can be observed. Finally, Fig.5 shows modal shape of the bearing at the frequency of 21700 Hz. In this figure, the 3-lobe shape of the bearing's bore is quite clear.

4.2. Second configuration

Figure 6 shows the second configuration of the acoustic journal bearing. Comparing to the first configuration, this one has thinner wall (1 mm in its middle section) and two conical rings at both ends. Both these features were introduced in order to make the bearing more pliable – an important factor for the generation of squeeze film acoustic pressure. Otherwise, the second configuration is quite similar to the first one with 30 mm nominal bore diameter and length of 50 mm. Aluminium alloy was used for the fabrication.

Elastic deformations of the bearing in radial direction are depicted in Fig. 7 while Fig.8 shows deformations of the bearing's bore. As in the case of the first configuration, three PZTs were attached to the outer surface of the bearing and the modulate current of 95 V was applied to them. Figure 9 illustrates modal shape of the bearing at the frequency of 48300 Hz. A 3-lobe shape can be easily observed.

4.3. Third configuration

The third configuration, shown in Fig.10, represents a radical departure from the previous two. The main features of this configuration are "elastic hinges "which main role is to provide maximum flexibility of the acoustic bearing. The bearing in the third configuration edition has the same bore diameter (30 mm) as the previous two but is significantly shorter with the length of 25 mm and is equipped with six PZTs (two at each slot shown in Fig.10). As in the case of the two previous configurations, aluminium alloy was used for fabrication. The way the bearing of the third configuration deforms in radial direction due to PZTs action at 95 V is shown in Fig.11. First observation to make is that deformation is much more pronounced and the original circular bore is transformed into distinct 3-lobe shape. Figure 12 depicts that in a very prominent way. Modal shape of the third configuration bearing at the frequency of 27200 Hz is illustrated in Fig.13. The desired 3-lobe shape is clearly visible.

5. Test apparatus and procedure

Experimental testing of the three configurations of the acoustic bearing was carried out using bespoke designed apparatus. Figure 14 schematically presents apparatus used for experimental testing of the bearing with squeeze film ultrasonic levitation. Essential and characteristic feature of the apparatus is the shaft vertically positioned and supported by an aerostatic thrust bearing placed on the base plate. This apparatus was especially designed and built to experimentally determine the load capacity of bearing's three configurations presented earlier. Shaft made of stainless steel had nominal diameter of 30 mm. Thrust bearing supporting the shaft and ensuring that it freely floats in the direction of its main axis was fed with compressed air supplied from an external source. Running of the shaft at speed was provided by an air turbine consisting of buckets machined circumferentially on the shaft and three air nozzles fixed to the housing and supplying air jets tangent to the shaft's

circumference. In this way a pure torque was applied to the shaft. Operation of PZTs and therefore the bearing tested was controlled by an amplifier and frequency generator. Position of the shaft within the journal bearing was measured in two planes by contactless sensors. The apparatus was clamped to the base plate and could be tilted by desired angle creating, in consequence, a loading on the bearing in a controlled way. The load on the bearing was calculated as a component of the shaft's weight determined by the tilt angle of the apparatus. Central objective of experimental testing was to determine the load capacity of three different configurations of the bearing by measuring the torque required to initiate shaft's rotation for given load on the bearing. That was carried out separately for PZTs switched on and switched off. Torque measurements were carried-out with the help of specially designed strain gauge beam shown in Fig. 15. It was calibrated as a function of gauge pressure of the air supplying the turbine driving the shaft.

Procedure of a typical test was as follows. First, it was required to ensure that the shaft was in true vertical position and floated freely on air cushion created by the aerostatic bearing fitted into the base of testing apparatus. Next, the offset voltage, usually, of 60 V was set so that the PZTs expanded and the bearing deformed accordingly. Following that, running voltage, corresponding to the amplitude of cyclic elastic deformations of the bearing, was adjusted to 50 V. As a result of rapid cyclic deformations of the bearing with the resonance frequency appropriate for the given bearing's configuration (found through modal analyses presented earlier) an air film was created separating shaft from the bearing due to the squeeze mechanism. For the stationary shaft the load carrying capacity of the air film created by the action of PZTs was ascertained by gradual tilting of the test apparatus base thus increasing the load on the bearing and measuring the torque required to initiate shaft's rotation. When there was an air film separating shaft from the bearing then the torque

required was quite minute constant till the maximum load capacity of the bearing was reached. Then, the torque initiating rotation of the shaft greatly increased because the air film thickness was insufficient to fully separate shaft from the bearing and, as a consequence, direct contact between the shaft and the bearing took place.

6. Experimental results and their discussion

Figure 16 shows how the driving torque required to initiate shaft's movement is changing with the increasing load on the bearing of first configuration. Initially, up to the load of 0.4 N, there is no difference between the bearing operating with PZT switched on and the one without PZT functioning. However, further increase in the load on the bearing required the increase in the torque to initiate shaft's rotation. The difference between the bearing aided by PZT and the one without that is very clear. Additionally, it is noticeable that the bearing of the first configuration (depicted in Fig. 2) does not have fully developed air film (judging by the magnitude of the torque) even though PZTs were switched on and operating at the resonance frequency of 58700 Hz. This is especially true for the loads greater than 0.8 N. In the case of the bearing without PZT on, the torque magnitude indicates a direct contact between the shaft and the bearing at loads greater than 0.8 N.

Performance of the bearing fabricated in accordance with the second configuration is shown in Fig. 17. Ability to support the load imposed on the bearing is quite similar to that of the first configuration, especially when PZTs are switched off. However, there is a slight improvement in the performance when the bearing operates with PZTs switched on. As it can be seen the torque remains constant and small even when the load on the bearing is 0.8 N. That was different in the case of the first configuration. Comparing to the first configuration, the second configuration makes the bearing more flexible. This is obvious

when comparing resonance frequencies for those two configurations. For that reason the bearing of second configuration seems to be able to support slightly higher loads.

Third configuration used to fabricate an acoustic test bearing is radically different from the previous two. Overall flexibility of the bearing, secured by "elastic hinges", is much higher comparing to the previous two configurations. This increased flexibility is evidenced by far better ability of the bearing to support the load (see Fig. 18). Up to the load of 1.2 N, the torque is small and constant suggesting a full separation of the interacting surfaces by an air film generated by the squeeze film acoustic levitation at the frequency of 8400 Hz.

Figure 19 shows performance of the same bearing but at higher resonance frequency of 34300 Hz. There are virtually no substantial differences between load capacity obtained when the bearing runs at 8400 Hz and 34300 Hz, apart from the fact that the low frequency is in an audible range.

7. Conclusions

The conclusions based on the results presented in this paper are as follows.

1. Results testify to the feasibility of the idea of a journal air bearing operating on a squeeze film acoustic levitation principle.

2. Geometric configuration of an acoustic bearing proved to be a very important factor governing the load supporting capacity.

3. Bearing possessing low overall stiffness which is provided by geometric configuration attested to much higher load capacity comparing to the other two configurations tested.

4. Increased flexibility of the bearing directly translates into bigger elastic deformation amplitude of the initially circular bore and hence improved ability to separate interacting

surfaces. This is only valid with the assumption that the force generated by PZT and responsible for elastic deformation of the bearing is kept constant.

8. References

[1] Stolarski, T.A., Self-lifting contacts – From Physical Fundamentals to Practical Applications, Proc. IMechE, Part C: J.Mech. Eng. Sci., 220 (2006), 1211-1218.

[2] Poynting, J.H. and Thomson, J.J., A textbook of Physics, Charles Griffin & Co., 1904.

[3] Daidzic, N., Nonlinear droplet oscillations and evaporation in an ultrasonic levitation, PhD thesis, Friedrich-Alexander University Erlangen, 1995.

[4] King, L.V., On the acoustic radiation pressure on spheres, Proc. R. Soc., London, 1934.

[5] Hasegawa, T., Acoustic radiation force on a solid elastic sphere, Acoustical Society of America, 46 (1969), 1139.

[6] Embleton, T.F.W., Mean force on a sphere in a spherical sound field, Acoustical Society of America, 26 (1954), 40.

[7] Westervelt, P.J., The mean pressure and velocity in a plane acoustic wave in a gas, Acoustical Society of America, 22 (1950), 319.

[8] Westervelt, P.J., The theory of steady forces caused by sound waves, Acoustical Society of America, 23 (1951), 312.

[9] Westervelt, P.J., Acoustic radiation pressure, Acoustical society of America, 29 (1957), 26.

[10] Gorkhov, L.P., On the forces acting on a small particle in an acoustical field in an ideal fluid, Soviet Physics Doklady, 6 (1962), 773.

[11] Barmatz, M. and Collas, P., Acoustic radiation potential on a sphere in plane, cylindrical, and spherical standing wave fields, Acoustical Society of America, 77 (1985), 928.

[12] Xie, W.J. and Wei, B., Dynamics of acoustically levitated disc samples, Physical Review, 70 (2004).

[13] Salbu, E.O.J., Compressible squeeze films and squeeze bearings, J. Basic Eng., 86 (1964) 355.

[14] Whymark, R.R., Acoustic field positioning for containerless processing, Ultrasonic, 13 (1975), 251.

[15] Wiesendanger, M., Squeeze film air bearing using piezoelectric bending elements, PhD thesis, Ecole Polytechnique Federale de Lausanne (2001).

[16] Stolarski, T.A. and Wei Chai, Load-carrying capacity generation in squeeze film action, Int. J. Mech. Sci., 48 (2006) 736.

[17] Hashimoto, Y., Transporting objects without contact using flexural travelling waves, Acoustical Society of America, 103 (1998), 3230.

[18] Warnock, L.F., Dynamic gas film supported inertial instrument, US Patent No. 3339421 (1967).

[19] Teitelbaum, B.R. and Farron, J.R., Squeeze film bearings, US Patent No. 3471205 (1969).

[20] Emmerich, C.L., Piezoelectric oscillating bearing, US Patent No. 3351393 (1967).

[21] Scranton, R.A., Planar and cylindrical oscillating pneumato-dynamic bearings, US Patent No. 4666315 (1987).

[22] Michael, W.A., A gas film lubrication study pt.II, IBM Journal, 1959, 286.

[23] Hamrock, B.J., Fundamentals of Fluid Film Lubrication, McGraw-Hill Co., 1994.

[24] Ide, T., Friend, J.R., Nakamura, K., and Ueha, S., A low-profile design for the noncontact ultrasonically levitated stage,, Japanese Journal of Applied Physics, 44 (2005), 4662.

[25] Yoshimoto, S., Anno, Y., and Hamanaka, K., Float characteristics of squeeze-film gas bearing with elastic hinges for linear motion guide, JSME International Journal, 40 (1997), 353.

[26] Stolarski, T.A., Performance of a self-lifting linear air contact, Proc. IMechE, Part C: J.Mech.Eng. Sci., 221 (2007), 1103.
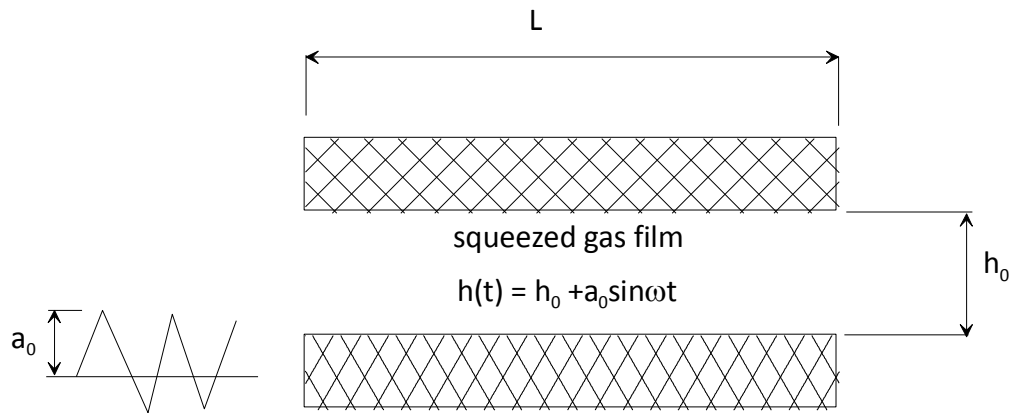
Figure 1. Schematic representation of the squeeze film levitation.
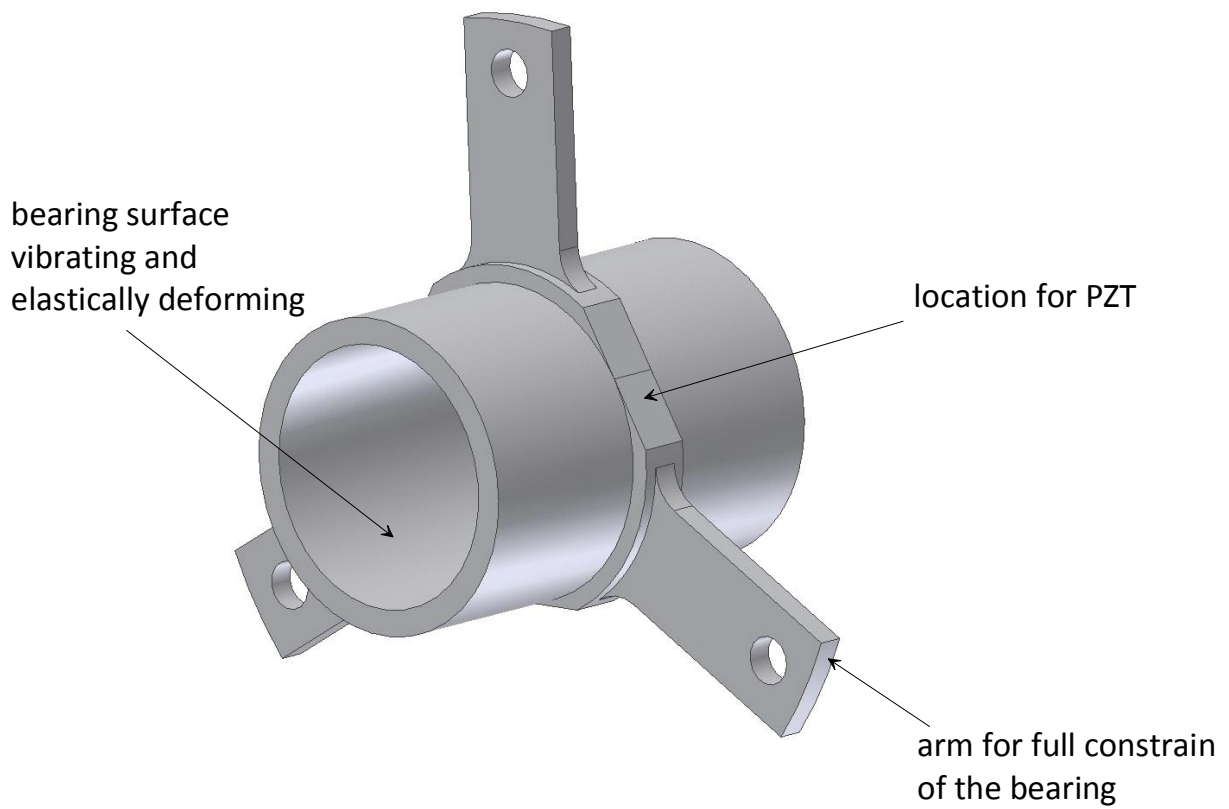
Figure 2. Solid model of the first configuration of acoustic bearing.

Figure(s)

NODAL SOLUTION
SUB =1
UX
RSYS=1
DMX =.753E-03
-.139E-03
-.394E-04
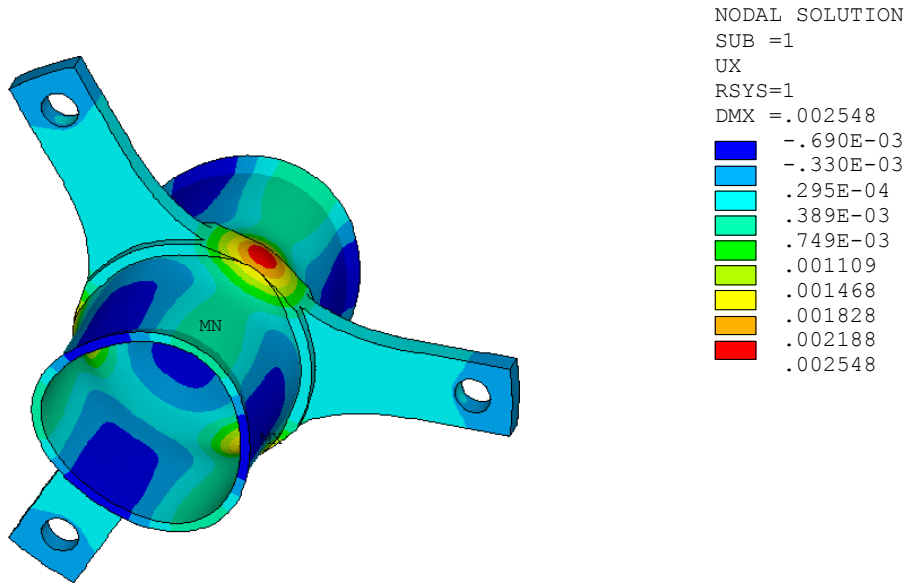.596E-04
.159E-03
.258E-03
.357E-03
.456E-03
.555E-03
.654E-03
.753E-03
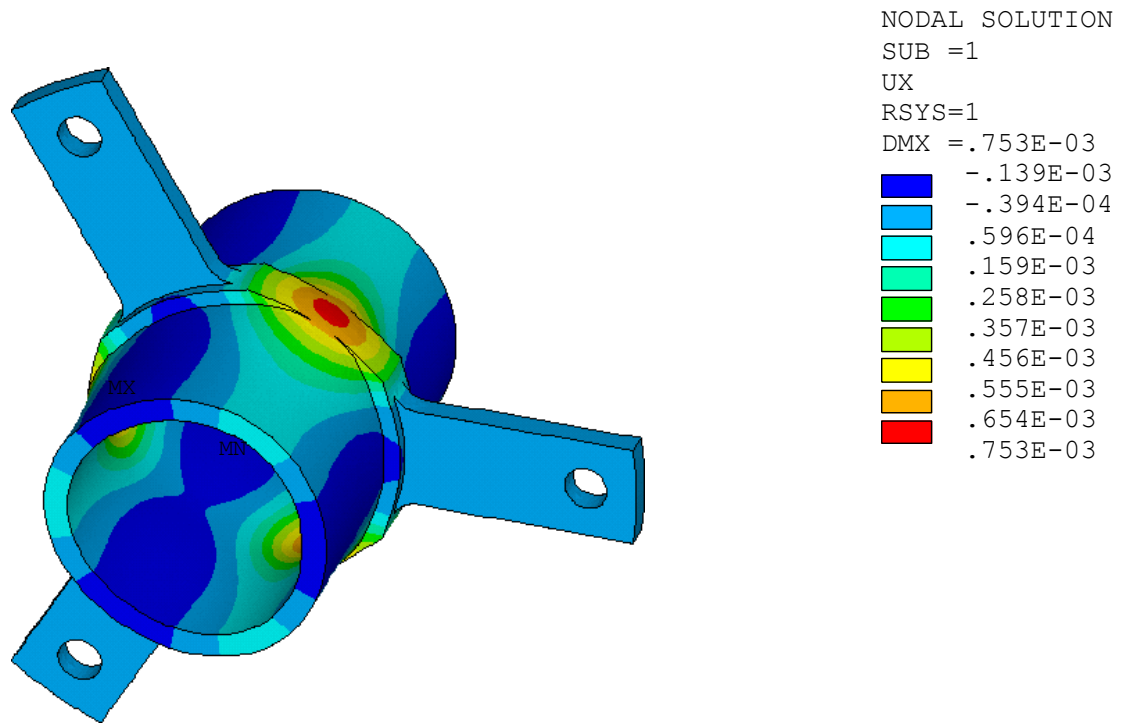
Figure 3. Radial elastic deformations of the bearing produced by PZTs powered by modulated current of 95 V (first configuration).
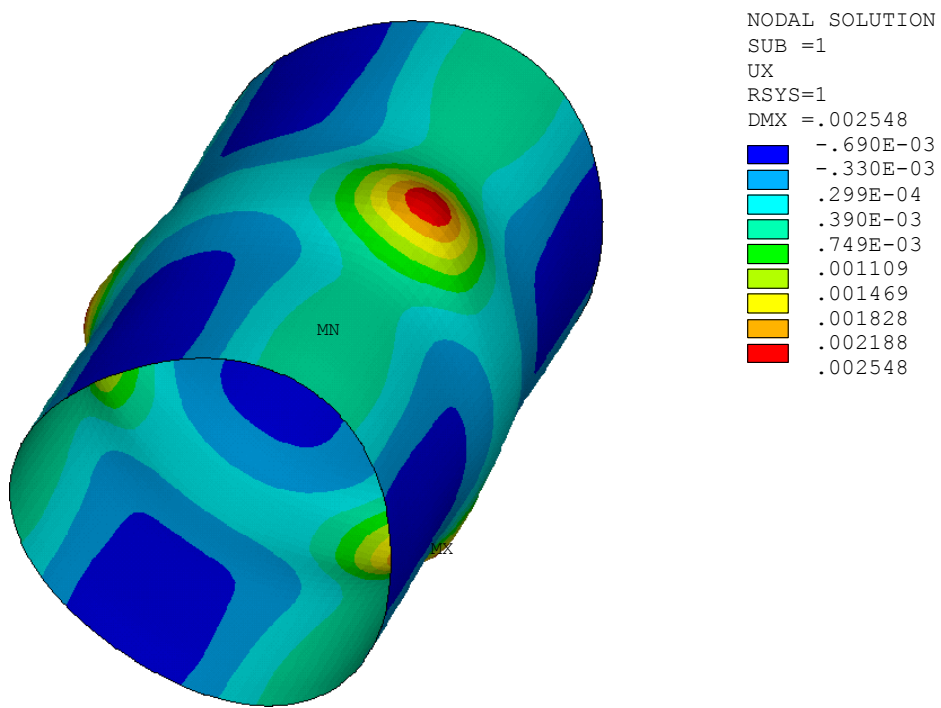

NODAL SOLUTION
SUB =1
UX
RSYS=1
DMX =.746E-03
-.136E-03
-.383E-04
.598E-04
.158E-03
.256E-03
.354E-03
.452E-03
.550E-03
.648E-03
.746E-03
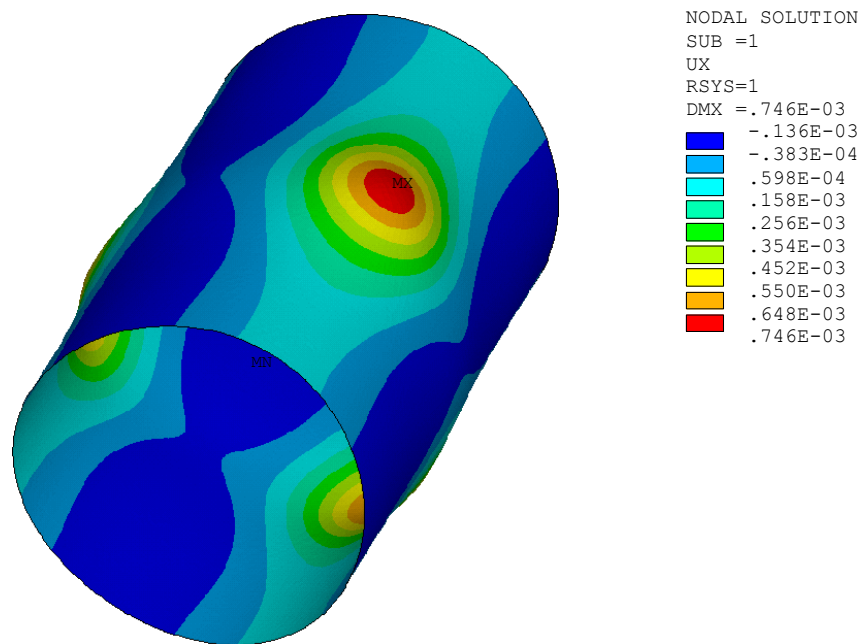
Figure 4. Amplified view of bearing's bore deformation (first configuration).

```
NODAL SOLUTION
SUB =13
FREQ=21783.5
UX
RSYS=1
DMX =333.286
     -332.108
     -258.309
     -184.51
     -110.712
     -36.9132
     36.8855
     110.684
     184.483
     258.281
     332.08
```
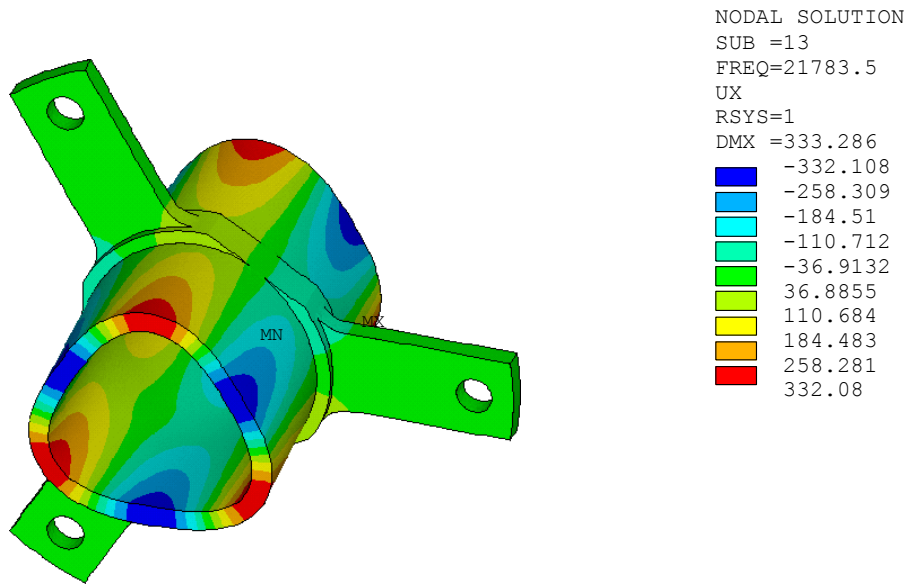
Figure 5. Modal shape of the bearing operating at the resonance frequency of 21700 Hz (first configuration).

bearing surface vibrating and elastically deforming
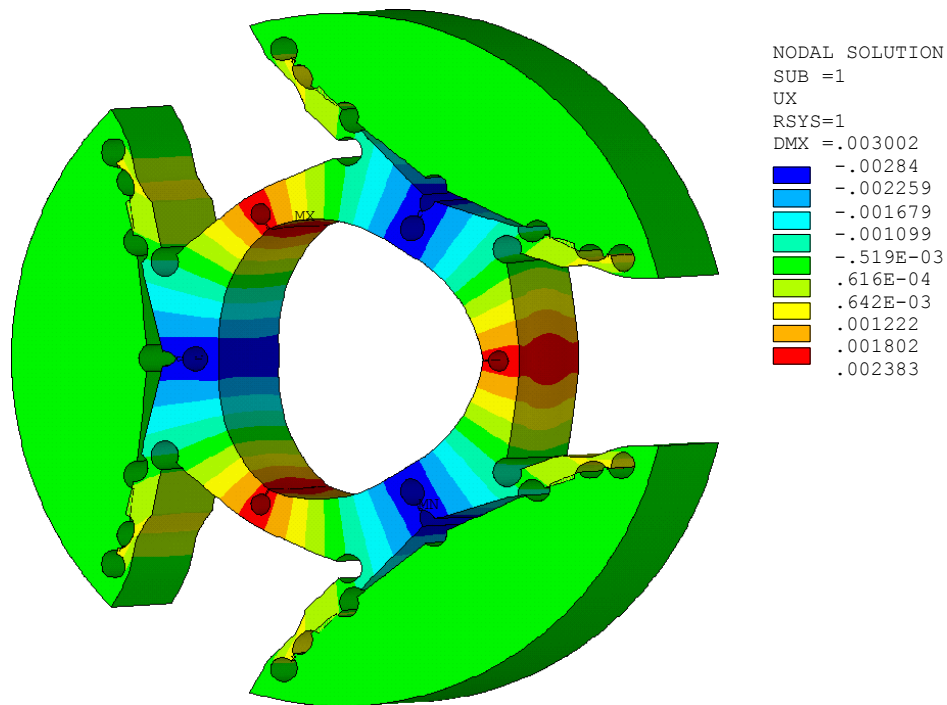
location for PZT

arm for full constrain of the bearing
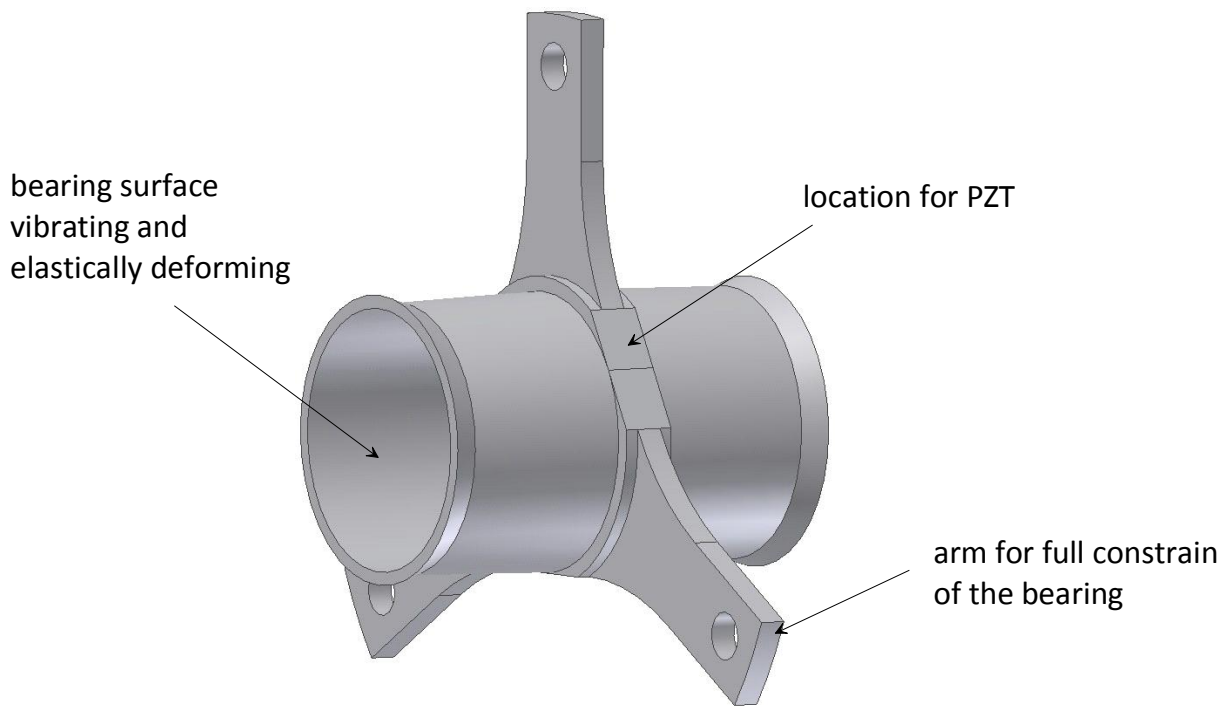
Figure 6. . Solid model of the second configuration of acoustic bearing.

Figure(s)

Figure 7. Radial elastic deformations of the bearing produced by PZTs powered by modulated current of 95 V (second configuration).
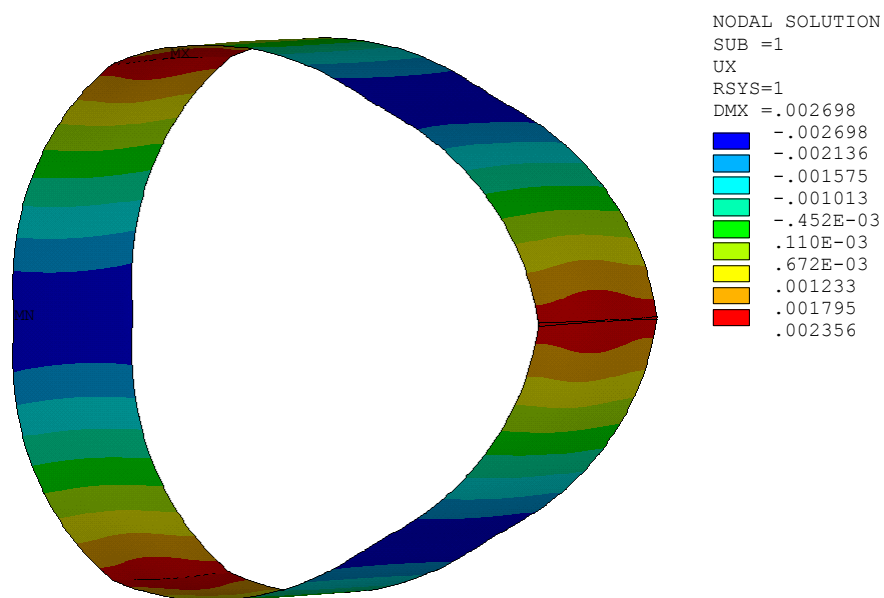

Figure 8. Amplified view of bearing's bore deformation (second configuration).

```
NODAL SOLUTION
SUB =100
FREQ=48272.5
USUM
RSYS=0
DMX =990.666
    1.46182
    111.373
    221.285
    331.197
    441.108
    551.02
    660.932
    770.843
    880.755
    990.666
```
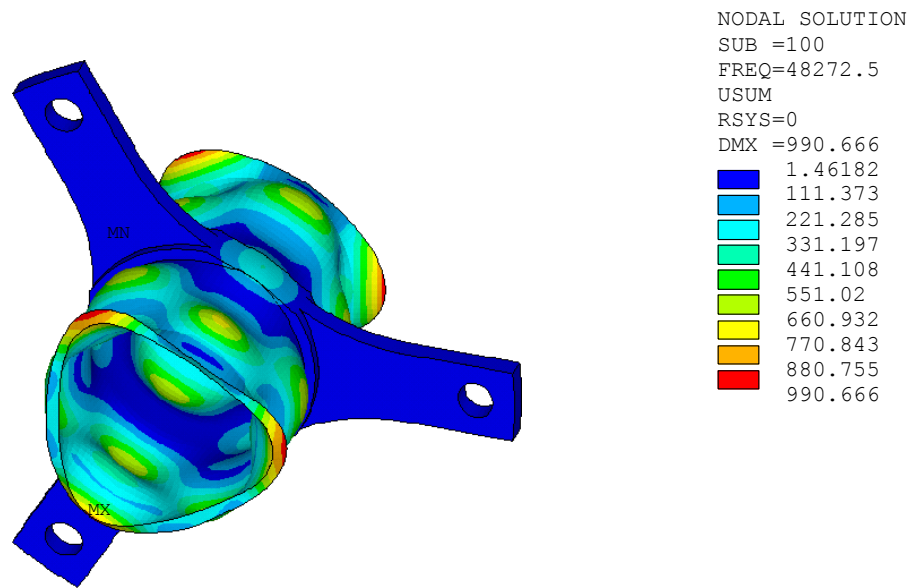
Figure 9. Modal shape of the bearing operating at the resonance frequency of 48300 Hz (second configuration).

fully constrained
outer surface

vibrating bearing surface
elestically deforming into
three-lobe configuration

slot for PZT

elastic hinge
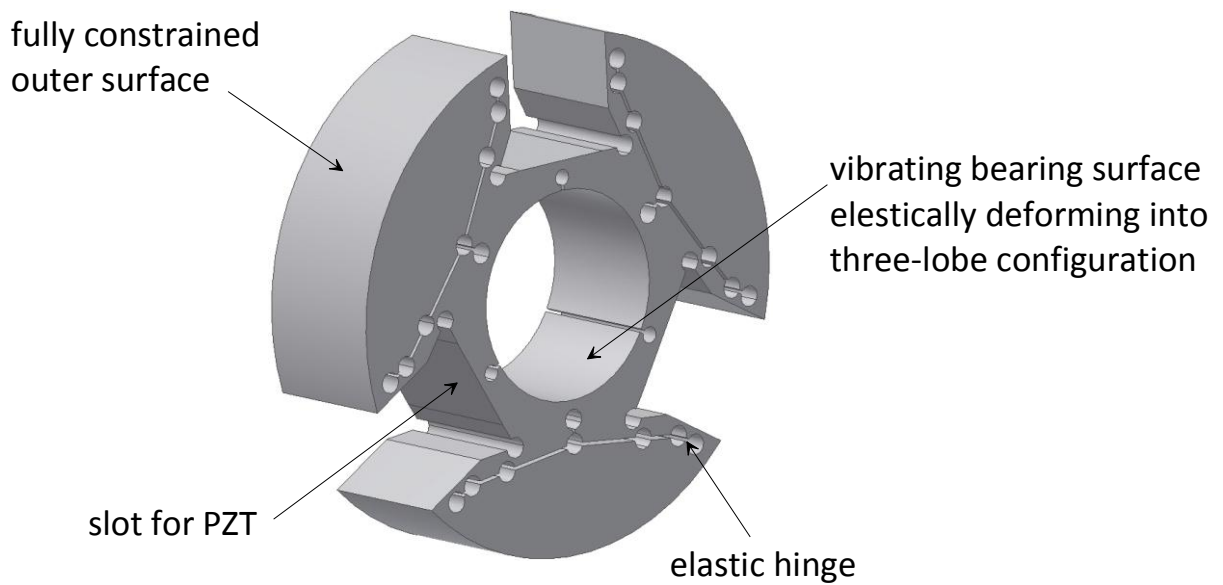
Figure 10. Solid model of the third configuration of acoustic bearing.

Figure 11. Radial elastic deformations of the bearing produced by PZTs powered by modulated current of 95 V (third configuration).

Figure 12. Amplified view of bearing's bore deformation (third configuration).
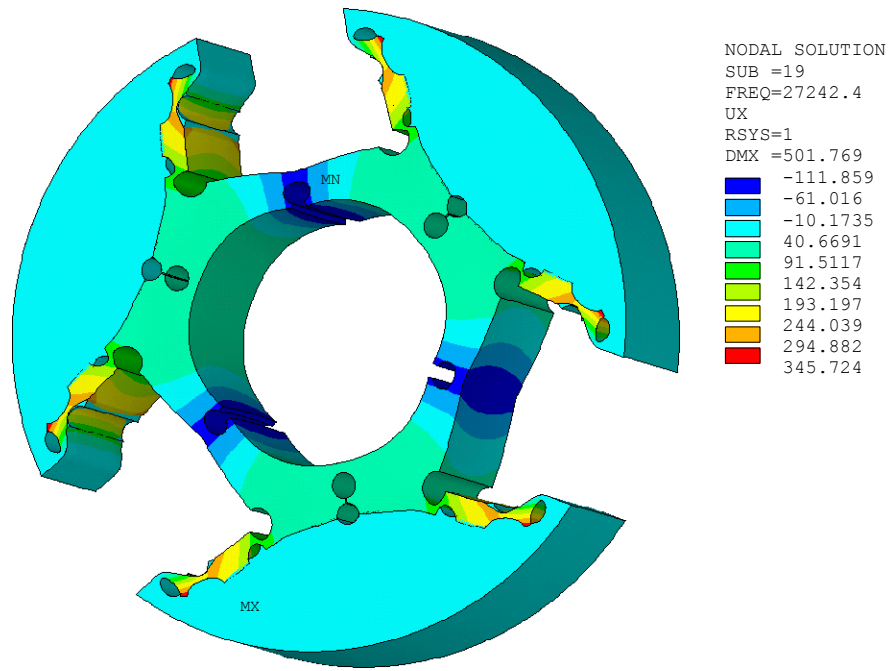
Figure 13. . Modal shape of the bearing operating at the resonance frequency of 27200 Hz (third configuration).
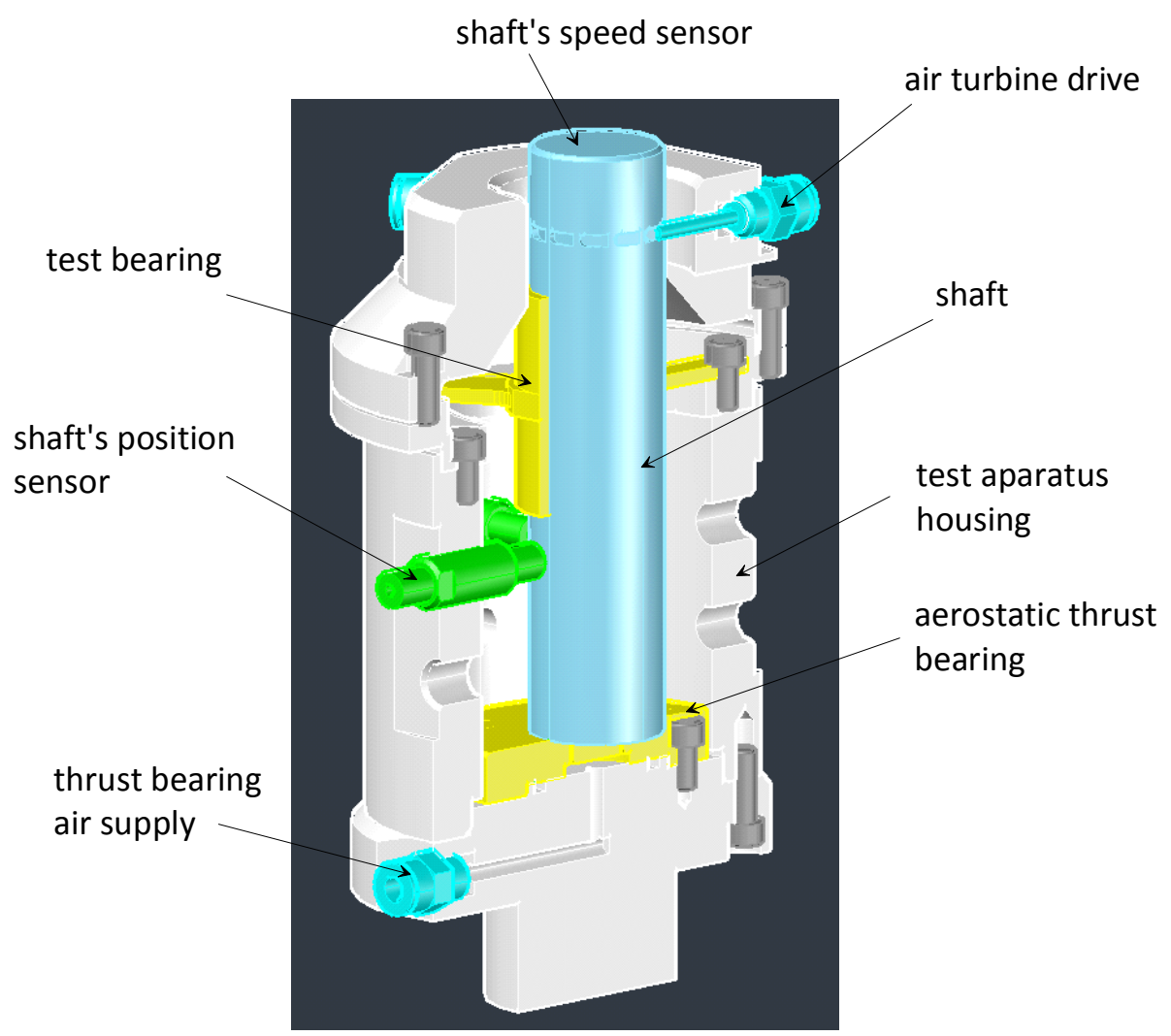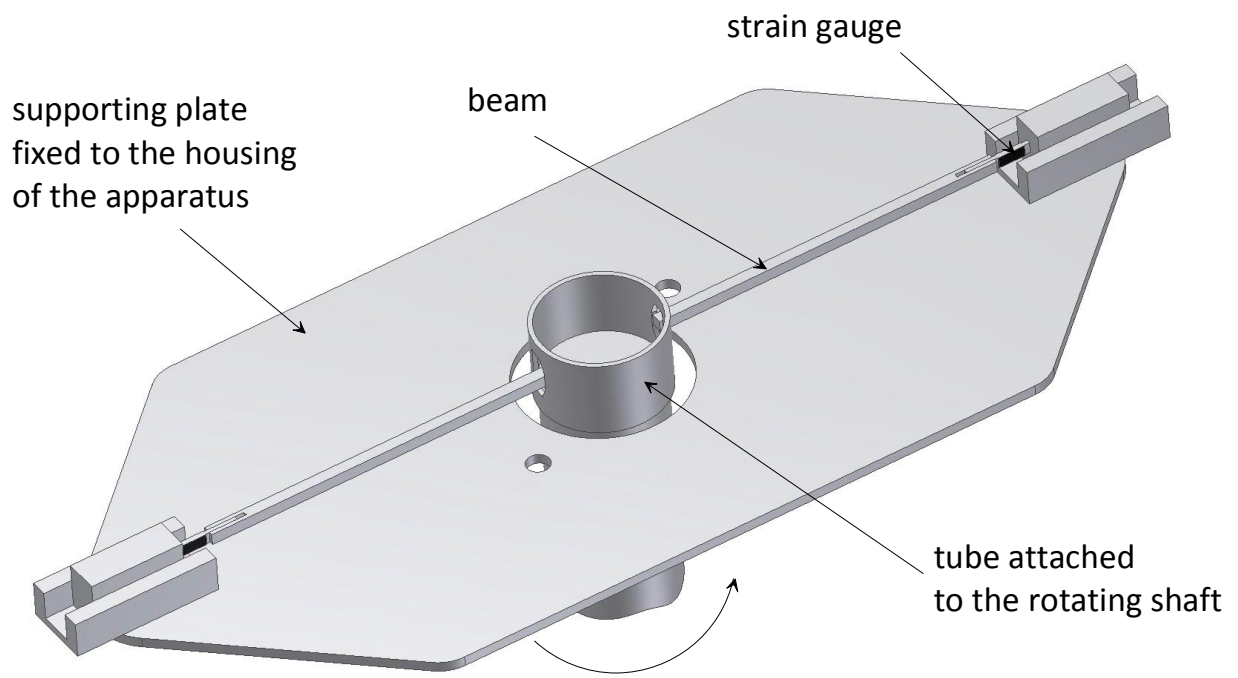
Figure 14. Solid model of the test apparatus.

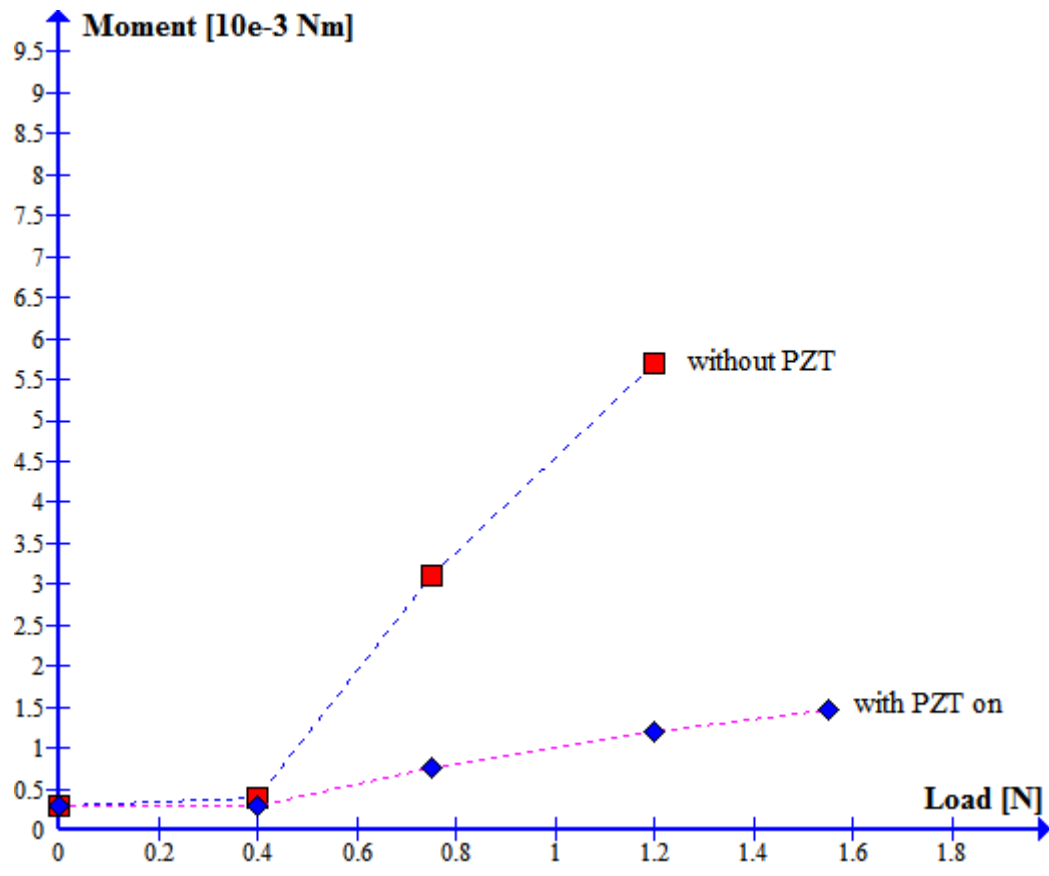Figure 15. Solid model of the device for torque measurements.

Figure 16. Driving torque as a function of the load applied to the bearing operating at 58700 Hz (first configuration is shown in Fig. 2).
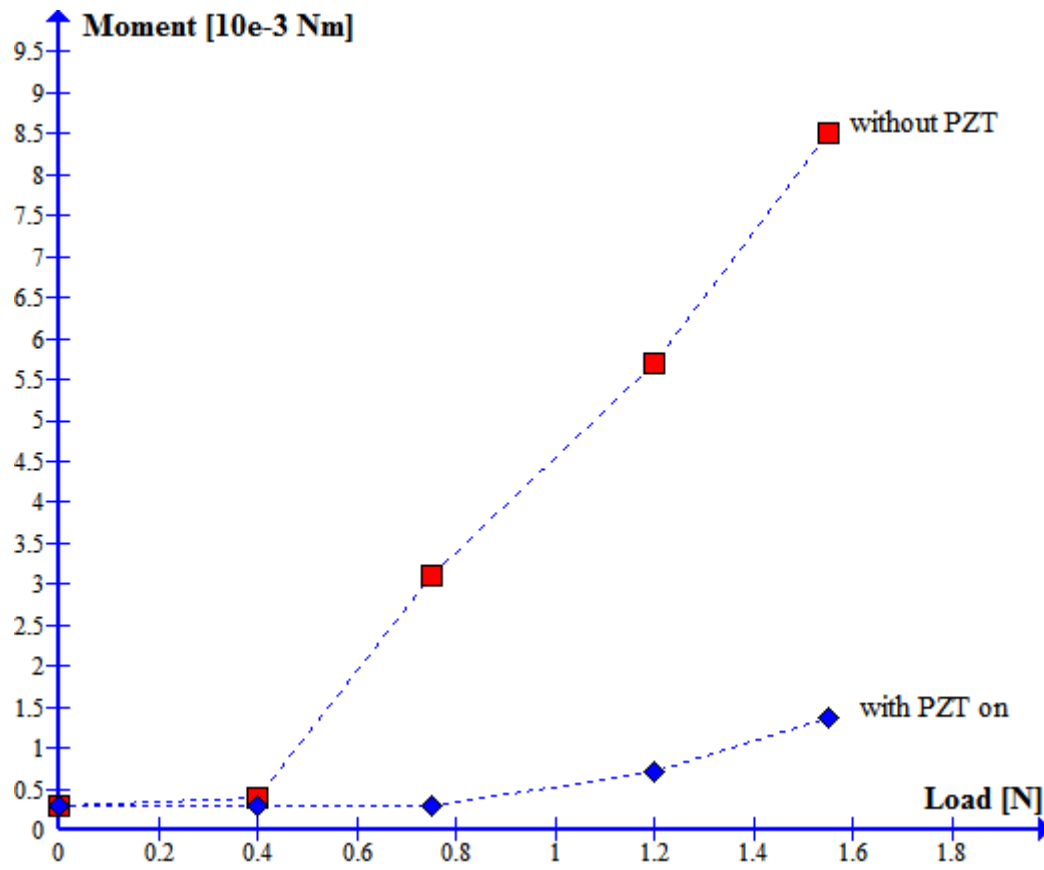
Figure 17. Driving torque as a function of the load applied to the bearing operating at 36700 Hz (second configuration is shown in Fig. 6).
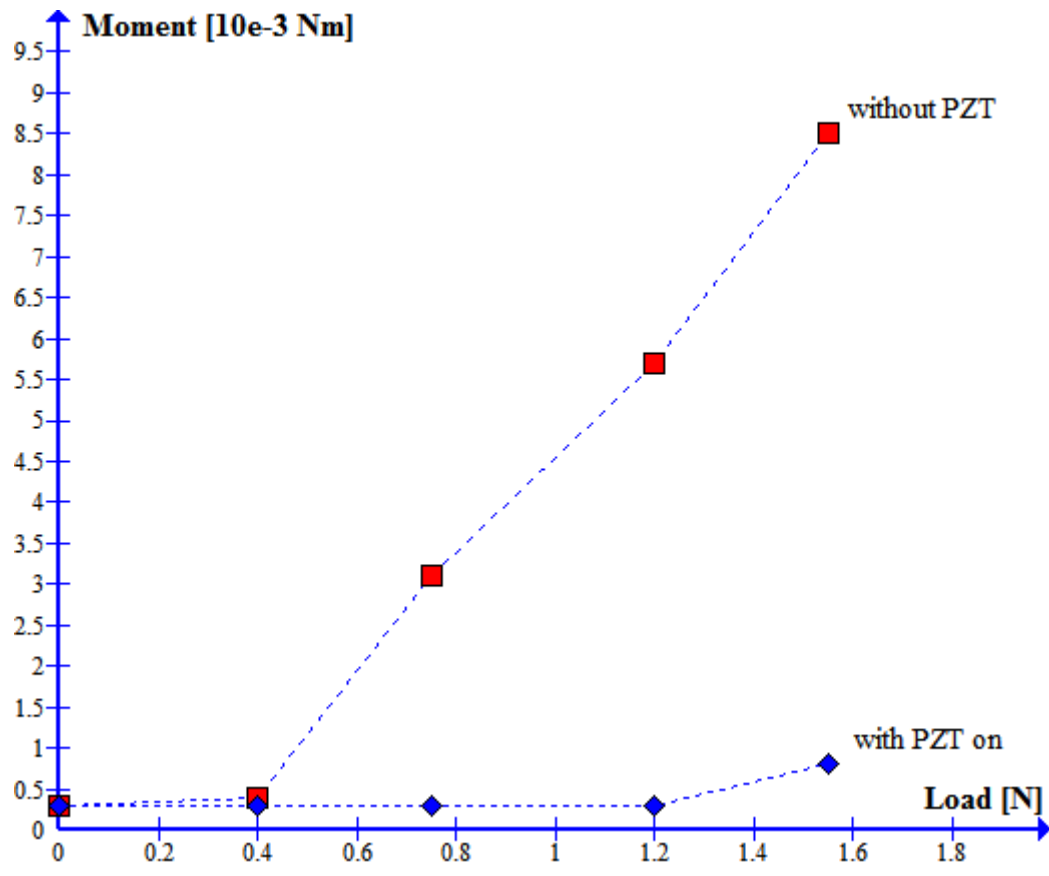
Figure 18. Driving torque as a function of the load applied to the bearing operating at 8400 Hz (third configuration is shown in Fig. 10).
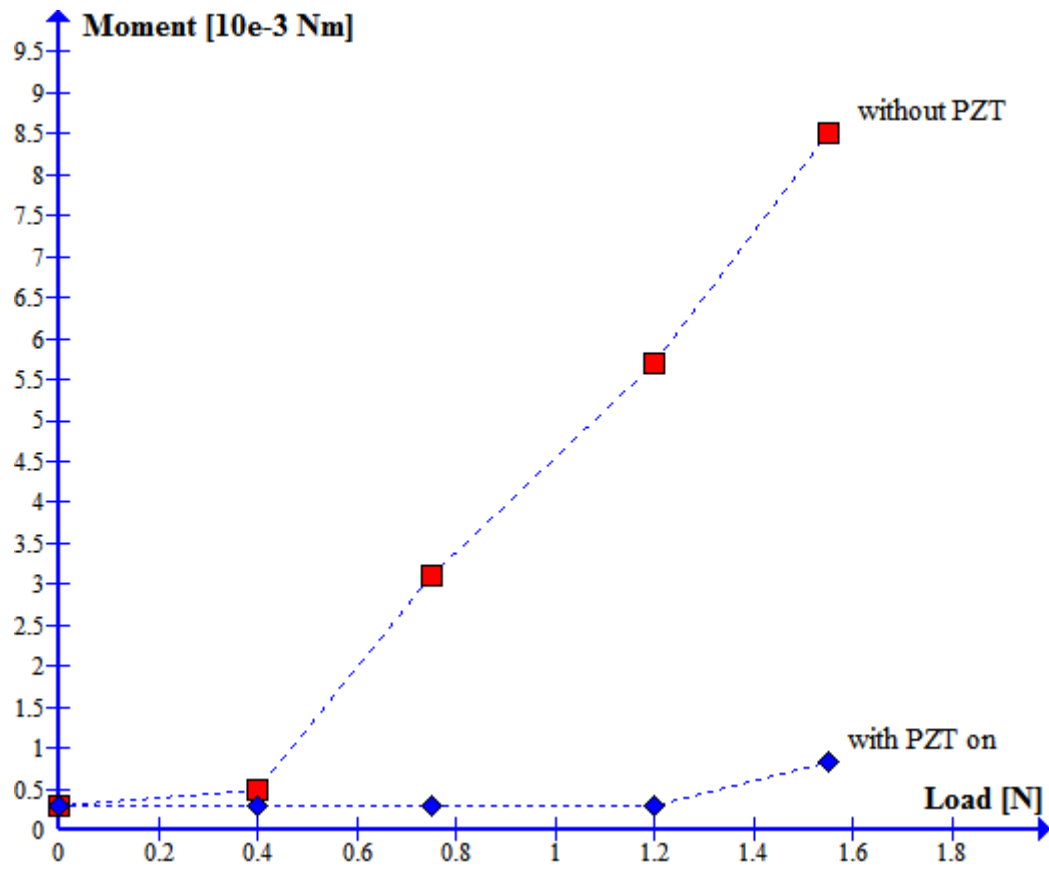
Figure(s)

Figure 19. Driving torque as a function of the load applied to the bearing operating at 34300 Hz (third configuration is shown in Fig. 10).